JOURNAL OF Applied Polymer SCIENCE

Investigation on Multifunctional Monomer Modified Polypropylene and Its Foamability

Wen Zhang,[1,2] Lili Yang,[1,2] Huaji Zhang,[1,2] Wei Lin,[3] Yuexiang Wang[3]

[1]College of Materials Science and Engineering, Fujian Normal University, Fuzhou 350007, China

[2]Fujian Key Laboratory of Polymer Materials, Fuzhou 350007, China

[3]Quanzhou Sansheng Rubber and Plastic Foamed Shoes Materials Co., Ltd, Quanzhou 362000, China

Correspondence to: W. Zhang (E-mail: zhangwen@fjnu.edu.cn)

ABSTRACT: 1,6-Hexanediol diacrylate (HDDA), pentaerythrithyl tetramethacrylate (PETMA), and triallyl-isocyanurate (TAIC) were used as representative monomers to modify polypropylene (PP) in the presence of dicumyl peroxide (DCP) in a mixer. Fourier transformed infrared spectroscopy (FTIR) results confirmed that all the three polyfunctional monomers have been grafted on PP backbone. The shape of torque curves suggested the occurrence of grafting and/or crosslinking structure. The rheological behaviors of HDDA modified PP showed the highest G' and lowest tan δ at low frequency, shear-thinning shifted to lower frequency in η^*–ω plot, as well as more deviation from semicircle characteristic of linear PP at high viscosity in Cole–Cole plot. And, the improvement of the mechanical properties followed the order as below: TAIC < PETMA < HDDA. Meanwhile, the foamability of the modified PP samples was also investigated. The cellular structure and morphology of the obtained foams were observed by scanning electron microscopy (SEM), and the results indicated that the foamability of the three modified PPs followed the same order, demonstrating HDDA modified PP foam possessed the highest cell density and expansion ratio, and the most well-defined closed cell structure and uniformly cellular morphology. © 2013 Wiley Periodicals, Inc. J. Appl. Polym. Sci. 000: 000–000, 2013

KEYWORDS: foams; viscosity and viscoelasticity; rheology; grafting; degradation

Received 31 January 2013; accepted 28 March 2013; Published online 00 Month 2013

DOI: 10.1002/app.39345

INTRODUCTION

The commercial polypropylene (PP) becomes a versatile thermoplastic after Ziegler–Natta discovery because of its desirable properties, such as high melting point and tensile modulus, low density and cost, as well as excellent chemical resistance. However, its highly linear chain structure and relatively narrow molecular weight distribution make it exhibit no strain hardening behavior in the molten state, leading to poor processing characteristics under elongational flow and limited applications in such fields as foaming, blow molding, extrusion coating, spinning and thermoforming.

To produce more value-added materials, much effort had been made to modify PP backbone by melt grafting,[1] electron beam irradiation,[2,3] and solid state grafting,[4–7] focusing on increasing the molecular weight and broadening the molecular weight distribution. Among these techniques, the melt grafting of PP through the recombination reactions between PP macromolecules and multifunctional monomers in the presence of an initiator to introduce long chain branching (LCB) had received much attention over the past decades.[8,9] During the melt grafting, the primary radicals generated by peroxide would abstract tertiary hydrogen preferentially, forming tertiary carbon macroradicals PP• which are unstable and easy to degrade through β-scission reactions. The purpose of the addition of polyfunctional monomer is to convert this active tertiary carbon PP• to the less lively secondary carbon PP•, favoring the recombination reactions rather than β-scission. Apparently, the selection of an appropriate polyfunctional monomer is one of the key factors to influence the mechanical properties of the modified PP. Zhang et al.[10] investigated the melt modification of PP with grafting monomers, *p*-(3-butenyl) styrene (BS), styrene (St), and divinylbenzene (DVB), in the presence of 2,5-dimethyl-2,5-di(tert-butylperoxy)hexane (DHBP). Compared with St and DVB, the usage of BS containing two double-bonds with different reactivity led to the formation of more uniformly distributed LCB structure on the PP backbone, and the resultant sample showed strain hardening in extensional flow and had high melt strength. Wan et al.[11] selected 2-(pyrrole-2-ylmethylene) malononitrile (PN), 2-(furan-2-ylmethylene) malononitrile (FN), and 2-cyano-3-(furan-2-yl)-2-propenoic acid ethyl ester (CFA) as monomers to modify PP in the molten state, and the

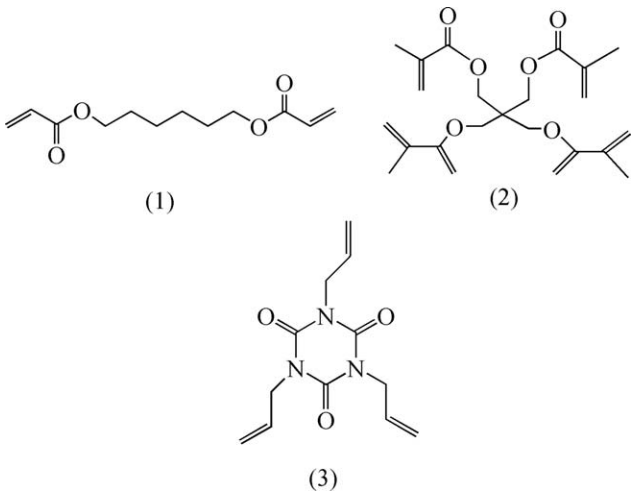

Figure 1. Molecular structure of monomers: (1) HDDA, (2) PETMA, and (3) TAIC.

results suggested that the chemical structures of both heteroaromatic ring and electron-attracting group played an important role in mediating macroradical reactions. FN modified PP owned the highest branching level and the most obvious elastic response which could be ascribed to the furan ring and the unusually reactive C=C bond resulted from the high electronegativity of cyano group.

In this article, three kinds of multifunctional monomer, bi-functional 1,6-hexanediol diacrylate (HDDA), tri-functional triallyl-isocyanurate (TAIC), and tetra-functional pentaerythrithyl tetramethacrylate (PETMA), were used to modify PP in the presence of dicumyl peroxide (DCP) in a mixer. The chemical structures of these monomers are presented in Figure 1. To evaluate the influence of these monomers on the melt radical functionalization of PP, small-amplitude oscillatory shear measurement was applied to investigate the linear viscoelastic behavior of these samples. Meanwhile, the foamability of the resultant PPs using azodicarbonamide (ADC) as the foaming agent were also studied and the characterization of the foams were presented based on cell density, expansion ratio, cellular structure, and average cell size.

EXPERIMENTAL

Materials

The co-PP used in this study, Versify 3000, was commercially obtained from Dow in granular form with *ca.* 5% ethylene content, a melt flow index (MFI) of 8 g/10 min (ASTM D1238, 230°C, 2.16 kg) and a density of 0.90 g/cm^3. The weight average molecular mass, $\bar{M}_w$, was 345,000, and $\bar{M}_w/\bar{M}_n = 4.32$. The three monomers, HDDA, PETMA, and TAIC, was supplied by Guangzhou Xinri Chemical Technology Co., Shanghai Aoke Industrial Co., and Hunan Yixiang Technology Co., respectively. Initiator DCP was offered by Akzo Nobel Cross-linking Peroxides (Ningbo). The chemical blowing agent ADC provided by Longyan Longhua Chemical Group is industrial grade and the decomposition temperature is 195°C. The nucleating agent, calcium carbonate ($CaCO_3$), was offered by Fujian Sannong Calcium Power Co. The blowing promoter, zinc oxide (ZnO), was supplied by Quanzhou Zhongtai Xinye Co. Antioxidant 1010 was obtained from Swiss Ciba Specialty Chemicals Co. Both xylene and acetone were reagent grade and used without further purification.

Preparation of Samples

The accurate weight of multifunctional monomer (1∼8 phr, phr represents part of agent per hundred parts of PP) and DCP (0.1 phr) were premixed and dissolved in a desired amount of acetone with 1:4 (volume ratio), then 45 g of PP and 0.09 g of antioxidant 1010 were also immerged in it. The mentioned mixture was stirred to make sure the additives dispersed well on the surface of PP resin, and then placed at room temperature until acetone volatilized completely. Finally, the modification of PP was conducted in an internal mixer (XSS-300, Shanghai Kechuang Rubber Plastics Machinery Set) at 160°C for 10 min with rotational speed of 60 rpm. The modified PP samples were denoted as M-x, in which M and x represents the multifunctional monomer and the number of phrs, respectively. For convenient comparison, both blank and control sample, which represented pure PP and PP with only 0.1 phrs of DCP, respectively, were obtained following the same process.

Purification of Modified PP

The purification of modified PP was carried out to remove any unreacted monomer and oligomer formed during the reaction for subsequent FTIR measurement. One gram of raw modified PP was dissolved in 80 mL refluxing xylene for 2 h and then poured into 120 mL acetone in hot immediately. The precipitate was filtered by Buchner funnel, washed by fresh acetone for three times and Soxhlet extracted in boiling acetone for 12 h to remove any soluble residues. Finally, the precipitate was dried at 80°C in an oven to a constant weight.

Preparation of PP Foam

The accurately weighted PP (100 phr) were introduced into an open mill (SXK 160 × 320 mm, GaoTie Seiki Enterprise Co.) at 110°C. After completely melting, $CaCO_3$ (25 phr), monomer (4 phr), ZnO (1 phr, blowing promoter), ADC (2 phr), and DCP (0.1 phr) were added in sequence and mixed for 10 min. A disk made from the obtained mixture was charged into a vulcameter (UR-2030SD, TaiWan YouKen Technology Co.) at 170°C for 10 min. Then, the mold was opened and the foams were taken out immediately. Moreover, both blank and control foamed samples were obtained following the same process.

Characterization

FTIR Analysis. Transmission FTIR spectra was recorded on a Nicolet 360-FTIR with a resolution of 4 cm^{-1}, and the scan range was from 4000 cm^{-1} to 400 cm^{-1} with a scan frequency of 32. The background was taken when the detector was exposed in the ambient environment.

Grafting Degree Determination. The grafting degree was determined by the carbonyl index (*CI*) which can be calculated as follows:

$$\mathrm{CI} = \frac{A_{\mathrm{C=O}}}{A_{1165}}$$

where $A_{(C=O)}$ is the absorbance of C=O in the monomer; and A_{1165} is the absorbance at 1165 cm^{-1} which was assigned to the

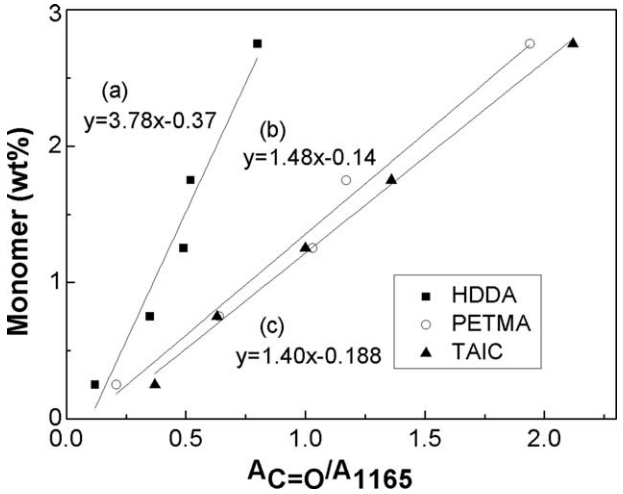

Figure 2. Calibration curves for determination of the weight percentage of grafted monomers in modified PPs: (a) HDDA, (b) PETMA, and (c) TAIC.

symmetric stretching vibration of CH_3 groups on PP backbone. According to Wan's method,[12] a series of the blends containing a certain amounts of monomer and PP were prepared in a mixer in the absence of DCP at 160°C for 10 min. Then, these samples were pressed into thin slices for FTIR measurement and the corresponding CI values were obtained. In Figure 2, the calibration curves presented the weight percentage of monomer plotted as a function of CI. According to these curves, grafting degree of modified PPs can be determined.

Gel Content Determination. The gel content of the modified PP was determined according to ASTM D2765. The sample was cut into small pieces, put into a 100-mesh copper bag and extracted with refluxing xylene at 130°C for 24 h. After extraction, the bag was dried in an oven at 80°C overnight to remove any residual solvent. The gel content was calculated as following:

$$\text{Gel content}(\%) = \frac{W}{W_0} \times 100\% \quad (1)$$

where W and W_0 is the exact weight of the sample after and before refluxing, respectively.

Rheological Characterization. The small-amplitude dynamic oscillatory shear measurement was carried out on a rotational rheometer (AR 2000, TA Instrument) with parallel-plate geometry (25 mm in diameter, 1 mm in the gap height) at 160°C. The frequency range was from 0.05 to 100 rad/s. The strain used was fixed at 1% which was confirmed to be within the linear viscoelastic region for all samples.

Cellular Structure Characterization. The cellular structure of the foams was observed by SEM (JSM-6380LV, JEOL). Samples were freeze-fractured in liquid nitrogen and made conductive by sputtering deposition of a thin layer of gold. SEM micrographs were taken from these fractured surfaces with a magnification of 50. The expansion ratio (v_a) of each sample was calculated by[13]:

$$v_a = \frac{\rho_p}{\rho_f} \quad (2)$$

where ρ_p and ρ_f is the bulk density of the original and foamed samples, respectively. ρ_f was measured via water displacement according to ASTM D1622-2008.

The cell density (N_0), the number of cells per cm^3 of the original polymer, was calculated by:

$$N_0 = \left(\frac{nM^2}{A}\right)^{\frac{3}{2}} \left(\frac{1}{1-V_f}\right) \quad (3)$$

where n is the number of cells observed in SEM micrographs, A is the area of the micrograph (cm^2), M is the magnification factor, and V_f is the void fraction of the foamed sample which can be determined by:

$$V_f = 1 - \frac{\rho_f}{\rho_p} \quad (4)$$

RESULTS AND DISCUSSION

FTIR Characterization and Grafting Degree Determination

Figure 3 showed that the FTIR spectra of PP and modified PPs after purification. For all the samples modified with HDDA, PETMA, and TAIC, there were band at about 1734, 1738, and 1694 cm^{-1}, respectively, which was attributed to the carbonyl (C=O) symmetric stretching vibration, indicating that the monomers had been grafted on PP backbone. Figure 4 presented the grafting degrees plotted as a function of the content of monomers. For these three monomers, all the grafting degrees increased with the addition of the monomer used, and with the same content of monomer, the grafting degree was increased with the order as follows: TAIC < PETMA < HDDA.

Torque Behavior Analysis

Figure 5(a) recorded the torque behaviors during the modification of PP with 4 phrs of monomers, while the blank and control experiments were also performed. For the blank PP, the torque curve leveled off after complete melting with 7.1 N·m of end-torque value. And, for the control PP, the torque decreased gradually after whole melt and reached 5.0 N·m, indicating that

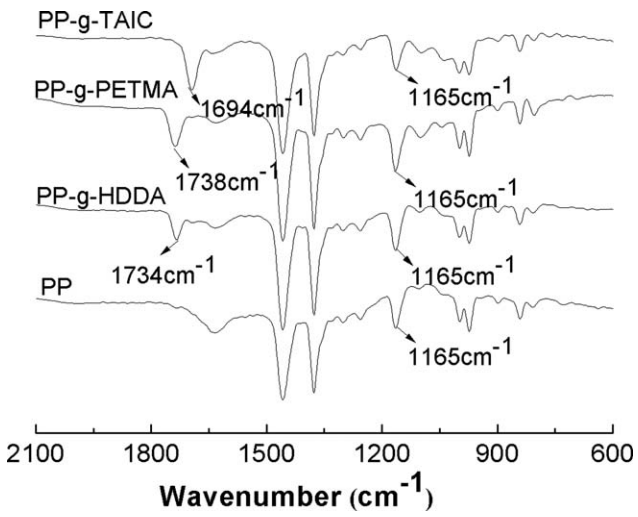

Figure 3. FTIR Spectra of modified PPs.

Applied Polymer SCIENCE

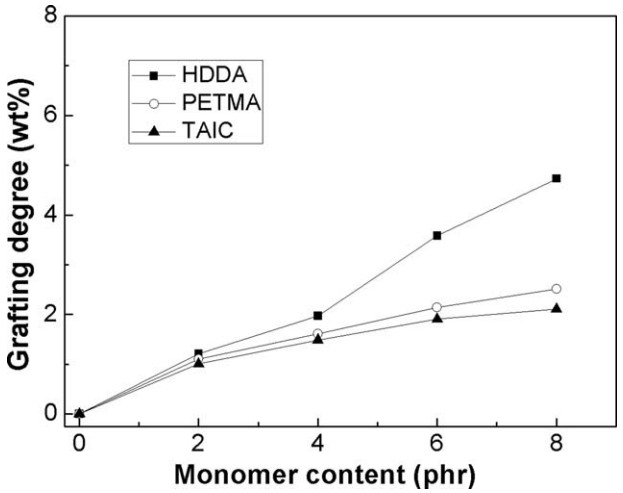

Figure 4. Effect of polyfunctional monomer on grafting degree of modified PPs.

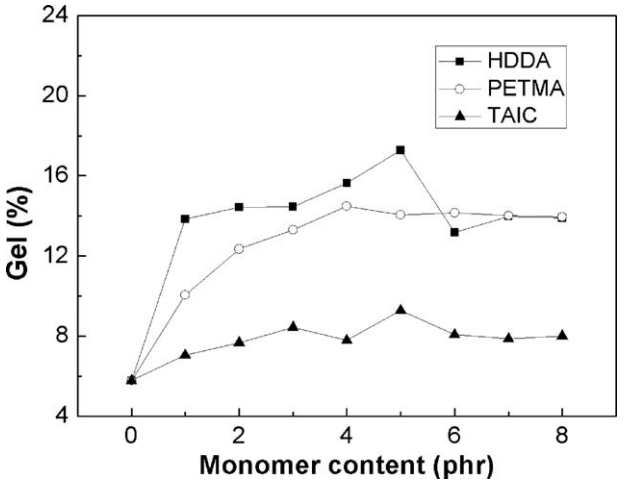

Figure 6. Effect of polyfunctional monomer on gel content of modified PPs.

severe degradation reaction of PP took place. However, when HDDA was added, there was a second peak started to appear at around 112 s, and the torque curve reached steady state with 6.8 N·m which was lower than that of the blank PP. According to Goodrich[14] and Maity,[15] if the process and formula are kept constant, the torque is proportional to the viscosity of polymer. Therefore, the second increase of the torque suggested the grafting and/or crosslinking reaction between PP• and HDDA•. With continued processing, HDDA was quickly depleted and β-scission exceeded the chain branching and/or crosslinking, leading to the decrease of torque value. When PETMA was used, the shape of curve remained the same as that of HDDA-4, while the end-torque value was 6.4 N·m which was lower than that of HDDA-4. This result might stem from the linear chain structure of HDDA which make it easy to penetrate into PP backbone,[16] resulting in more grafted and/or crosslinked PP. In the case of TAIC, there was no second torque peak and the end-torque value was 5.8 N·m, the lowest one among the three data. On the basis of the previous literatures, the strong electron withdrawing nature of isocyanuric ring would lower the electron density of allyl radical of TAIC[17] and weaken the reactivity of TAIC with PP•. On the other hand, the polar groups (–NCO) might decrease the dispersion of TAIC in PP matrix, reducing the reaction probability between PP• and TAIC.[16] Simultaneously, the steric hindrance[17] of TAIC would also confine the formation of branching and/or crosslinking structure along the PP backbone.

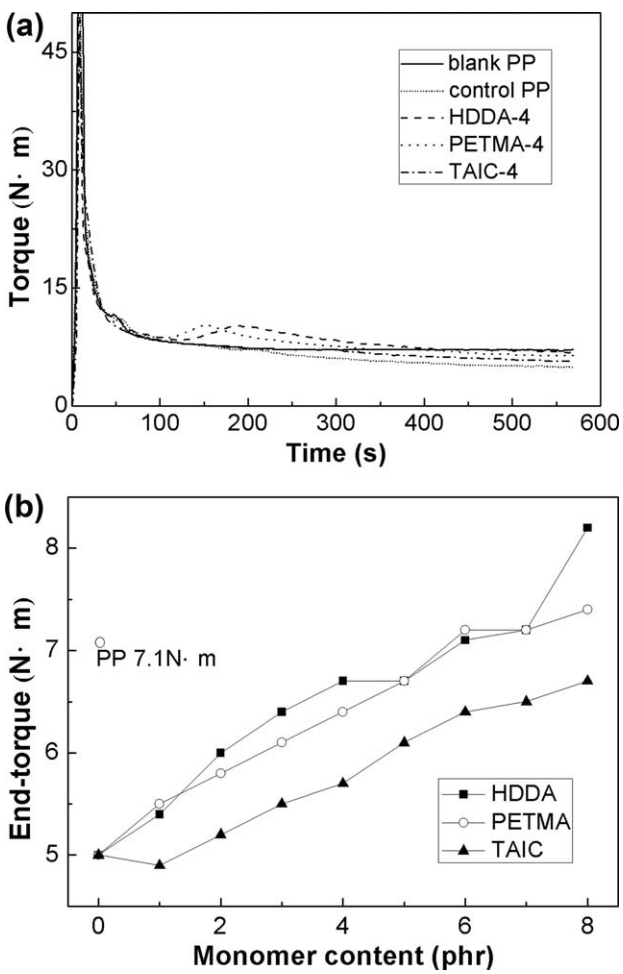

Figure 5. (a) Torque behavior during the functionalization runs of PP with polyfunctional monomers. (b) Effect of polyfunctional monomer on end-torque value of modified PPs.

In Figure 5(b), the end-torque values of the samples were increased with the addition of the monomers. Especially, in the condition of HDDA and PETMA content beyond 6 phr, the end-torque values surpassed that of the blank PP, suggesting that the viscosity of HDDA and PETMA modified PP was improved obviously.

Gel Content Determination

The effect of multifunctional monomer content on gel content was shown in Figure 6. The gel content of control PP was determined with 5.8%, which was come from the recombination reactions between secondary macroradicals located on polyethylene units of PP. At a given amount of peroxides, all the gel content increased with the addition of monomer content, and reached the maximum of 17.3, 14.5, and 9.3% for HDDA,

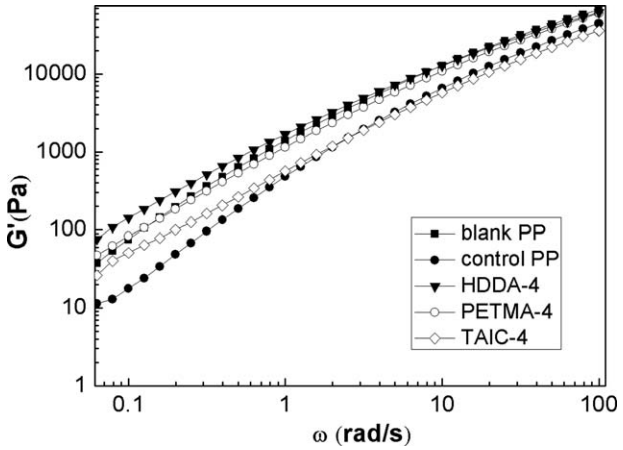

Figure 7. Storage modulus versus angular frequency for the modified PPs.

PETMA, and TAIC, respectively. For further increasing the monomer content, the gel content of PETMA and TAIC modified PP kept stable, while the value of HDDA modified PP decreased. For the former case, too much monomer cannot give rise to more crosslinking reaction because the active sites on the PP backbone initiated by a given amount of peroxide were saturated. However, due to the linear structure of HDDA, too high content of monomer make it easy not only to recombine with PP• to form short branching chains, but also to react with each other to produce homopolymer. Therefore, the formation of these byproducts consumed largely the monomers which were used to stabilize tertiary carbon macroradicals and inhibit β-scission reaction, giving rise to PP degradation and gel content decrease.

Rheological Characterization

The change of storage modulus at low frequency, reflecting the difference of relaxation time, is very sensitive to the topological structure of macromolecules. The dynamic storage modulus (G') curves of modified PPs were displayed in Figure 7. The blank PP exhibited characteristic behavior of linear viscoelastic material in the Newtonian (terminal) region. For the control PP, the terminal slope of the G' (ω) curve and the modulus over the whole frequency range were lower than that of the

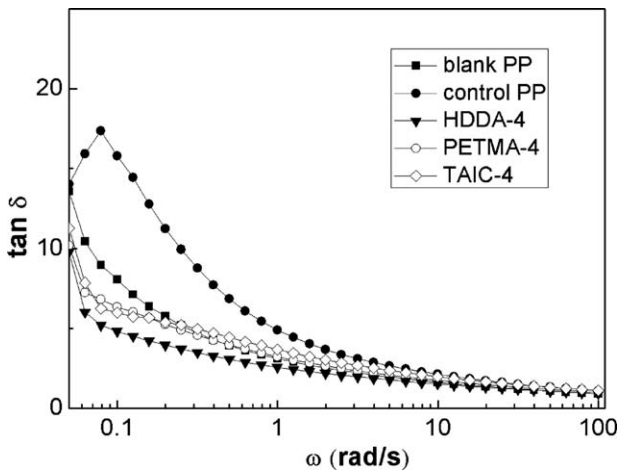

Figure 8. Tan δ versus angular frequency for the modified PPs.

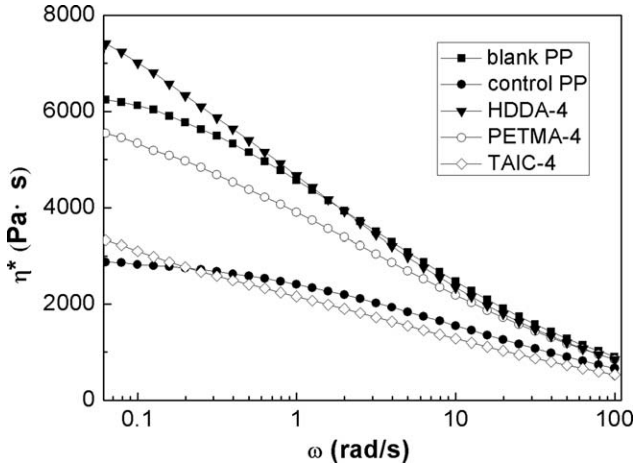

Figure 9. Complex viscosity versus angular frequency for the modified PPs.

blank PP. The observation was in accordance with the results obtained by Zhang[9] who assigned this phenomenon to the presence of low molecular linear chains. G' of all the modified samples at low frequency were higher than that of the control PP, especially in the case of HDDA-4 and PETMA-4, the values were even higher than that of the blank PP and the slopes also deviated from the terminal behavior of blank PP, indicating that there is a longer relaxation mechanism which can be ascribed to more branching and/or crosslinking.

Figure 8 showed tan δ as a function of angular frequency. With the decreasing frequency, tan δ of the blank PP was ascending. Within the whole tested frequency, tan δ of the control PP was higher than that of blank PP and there was a small peak at low frequency which was in accordance with Zhang's results,[9] owing to the existence of chain scission and/or microgel. In the presence of multifunctional monomers, all the values were lower than that of blank PP at low frequency and varied with the types of monomers used. This was attributed to the formation of branching and/or crosslinking structure which will result in different terminal relaxation time.[11,18,19]

The complex viscosity (η^*) is extremely sensitive to branching and/or crosslinking structure and the presence of very low

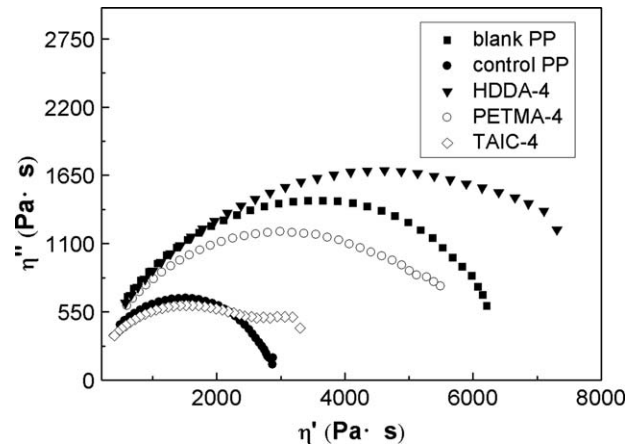

Figure 10. Cole–Cole plot for the modified PPs.

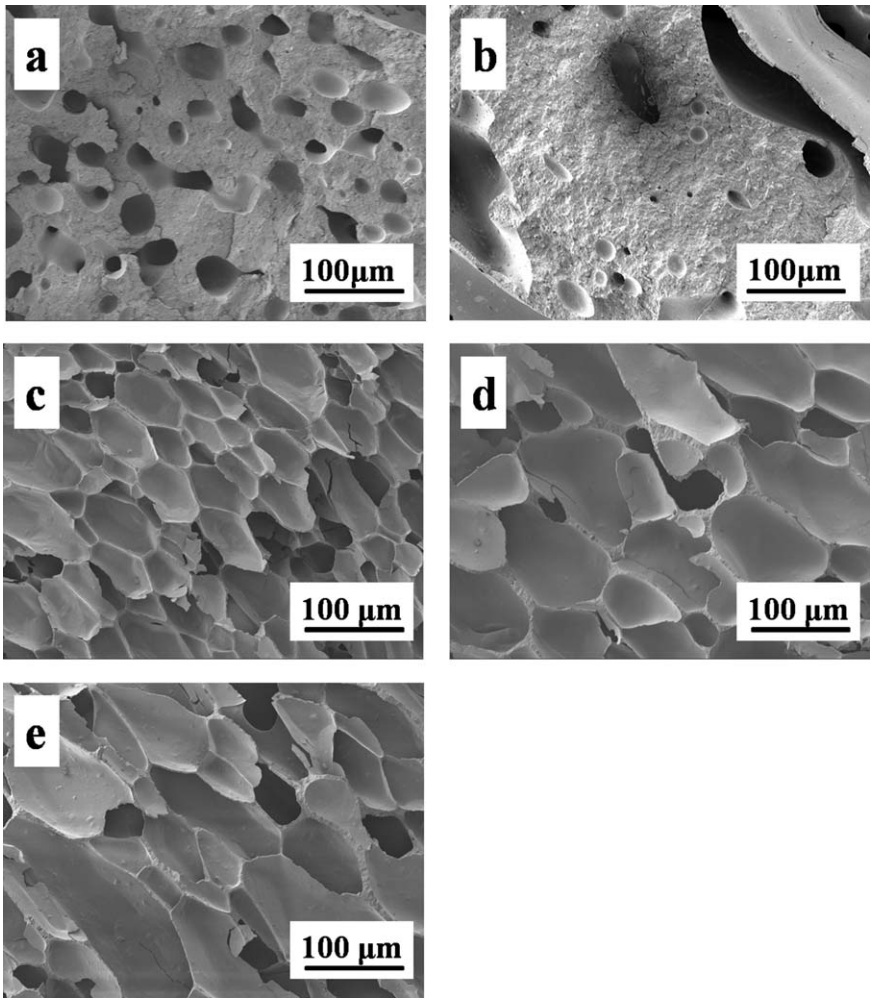

Figure 11. SEM micrographs for foamed samples: (a) blank PP, (b) control PP, (c) HDDA-4 modified PP, (d) PETMA-4 modified PP, and (e) TAIC-4 modified PP.

amounts of branching and/or crosslinking can change the degree of shear thinning compared with the linear polymer with similar molecular weight.[20–22] In Figure 9, the curve of the blank PP showed a plateau at low frequency, which was in good agreement with the typical shape of the linear polymer.[8,9,23] Compared with blank PP, η^* of the control PP declined more severely and the Newtonian-zone became broader, implying that β-scission took place and the molecular weight decreased. In the presence of monomers, all the complex viscosity curves were higher than that of the control PP and the transitions from Newtonian-plateau to shear-thinning region were shift to lower frequency. Especially, in the case of HDDA, the value was higher than that of the blank PP. And, the shear-thinning behavior of HDDA-4 was the most distinct among all the three samples, these observation were in accordance with Langston's result,[20] which was attributed to longer relaxation time of branched and/or crosslinked polymers.

Table I. Information About Modified PP Foam

Code	ρ_f (g/cm^3)	v_a	Average cell size (μm)	N_O (cell/cm^3)
HDDA-4	0.176	5.0	256	4.62×10^{10}
PETMA-4	0.191	4.61	439	1.25×10^{10}
TAIC-4	0.224	3.93	486	5.2×10^{9}

Figure 10 presented Cole–Cole plot of the modified PPs. For the blank and control PP, the Cole–Cole plots were close to a semicircle and the higher the molecular weight, the larger the radius.[23] The curves of PETMA-4 and TAIC-4 located between that of the blank PP and control PP, indicating that the degradation reaction also took place, but the degradation degree was restrained to a certain degree. However, the curve of HDDA-4 was higher than that of the blank PP and showed evidently a deviation from semicircle, suggesting the most branching and/or crosslinking involved, and finally the longest relaxation time.[7,24]

Morphological Characterization

Figure 11 presented the SEM micrographs of the cross-section of cryofractured samples and the detailed data were shown in Table I . In Figure 11(a), blank PP displayed the typical cell morphology of low melt strength PP, such as open cell structure and large unfoamed regions. Compared with the blank PP

foam, the control PP foam [Figure 11(b)] showed much more unfoamed regions as a result of lower melt strength, which makes it difficult to hold gas within the melt. With the highest N_0 (1.03×10^{10} cell/cm^3) and v_a (5.0), HDDA-4 modified PP foam [Figure 11(c)] displayed well-defined closed cell structure and uniformly cellular morphology with the smallest average cell size (256 μm). However, in the PETMA-4 and TAIC-4 involved system [Figure 11(d,e)], the larger cell structures and more irregular-shaped cells were obtained, especially for the latter one, suggesting the occurrence of cell coalescence and collapse during foam expansion. Compare with HDDA-4, relative lower melt strength and poorer melt elasticity make the cell walls not strong enough to bear the internal gas pressure and rupture more easily, resulting in the lower cell density and expansion ratio, as well as larger average cell size.[25,26]

CONCLUSION

In this article, the influences of three different polyfunctional monomers on the mechanical properties of modified PP in the presence of DCP were investigated. FTIR analysis confirmed the graft of polyfunctional monomers on PP backbone. The dependence of torque on processing time indicated that the presence of polyfunctional monomers favored the formation of the grafting and/or crosslinking structure and HDDA modified PP presented the best melt viscosity among the three monomer involved systems. Meanwhile, the rheological behaviors of HDDA modified PP also showed the highest G' and lowest tan δ at low frequency, shear-thinning shifted to lower frequency in η^*-ω plot, as well as more deviation from semicircle characteristic of linear PP at high viscosity in Cole–Cole plot. The mechanical properties of modified PP improved with the sequence as: TAIC < PETMA < HDDA. Also, the foamability of the three modified PPs followed the same order, indicating that HDDA modified PP foam obtained the most well-defined closed cell structure and uniformly cellular morphology with the highest cell density and expansion ratio, as well as the smallest average cell size.

ACKNOWLEDGEMENTS

Financial support from the Education Department of Fujian Province (JK2011011, JB12024) is gratefully acknowledged.

REFERENCES

1. Moad, G. *Prog. Polym. Sci.* **1999**, *24*, 81.
2. Han, D. H.; Jang, J. H.; Cho, B. G.; Kim, B. N.; Seo, G. S. *Polymer*, **2006**, *47*, 6592.
3. Yoshii, F.; Makuuchi, K.; Kikukawa, S.; Tanaka, T.; Saitoh, J.; Koyama, K. *J. Appl. Polym. Sci.* **1996**, *60*, 617.
4. Rätzsch, M.; Arnold, M.; Borsig, E.; Bucka, H.; Reichelt, N. *Prog. Polym. Sci.* **2002**, *27*, 1195.
5. Patel, A. C.; Brahmbhatt, R. B.; Rao, P. V. C.; Rao, K. V.; Devi, S. *Eur. Polym. J.* **2000**, *36*, 2477.
6. Zhang, L. F.; Guo, B. H.; Zhang, Z. M. *J. Appl. Polym. Sci.* **2002**, *84*, 929.
7. Borsig, E.; van Duin, M.; Gotsis, A. D.; Picchioni, F. *Eur. Polym. J.* **2008**, *44*, 200.
8. Xing, H. P.; Jiang, Z. W.; Zhang, Z. J.; Qiu, J.; Wang, Y. H.; Ma, L.; Tang, T. *Polymer*, **2012**, *53*, 947.
9. Zhang, Z. J.; Wan, D.; An, Y. J.; Liu, F.; Xing, H. P.; Wang, L.; Jiang, Z. W.; Tang, T. *Polym. Degrad. Stab.* **2011**, *96*, 653.
10. Zhang, Z. J.; Wang, D.; Xing, H. P.; Zhang, Z. J.; Tan, H. Y.; Wang, L.; Zheng, J.; An, Y. J.; Tang, T. *Polymer*, **2012**, *53*, 121.
11. Wan, D.; Ma, L.; Xing, H. P.; Wang, L.; Zhang, Z. J.; Qiu, J.; Zhang, G. C.; Tang, T. *Polymer*, **2013**, *54*, 639.
12. Wan, D.; Ma, L.; Zhang, Z. J.; Xing, H. P.; Wang, L.; Wang, L.; Jiang, Z. W.; Zhang, G. C.; Tang, T. *Polym. Degrad. Stab.* **2012**, *97*, 40.
13. Kumar, V.; Suh, N. P. *Polym. Eng. Sci.* **1990**, *30*, 1323.
14. Goodrich, J. E.; Porter, R. S. *Polym. Eng. Sci.* **1967**, *7*, 45.
15. Maity, A. K.; Xavier, S. F. *Eur. Polym. J.* **1999**, *35*, 173.
16. Su, F. H.; Huang, H. X. *J. Appl. Polym. Sci.* **2010**, *116*, 2557.
17. Matsumoto, A.; Kubo, T.; Watanabe, K.; Aota, H.; Takayamab, Y.; Kameyamab, A.; Nakanishib, T. *Eur. Polym. J.* **2000**, *36*, 673.
18. Graebling, D. *Macromolecules*, **2002**, *35*, 4602.
19. Gotsisa, A. D.; Zeevenhoven, B. L. F. *J. Rheol.* **2004**, *48*, 895.
20. Malmberg, A.; Gabriel, C.; Steffl, T.; Munstedt, H.; Lofgren, B. *Macromolecules* **2002**, *35*, 1038.
21. Langston, J. A.; Colby, R. H.; Mike Chung, T. C. *Macromolecules* **2007**, *40*, 2712.
22. Romani, F.; Corrieri, R.; Braga, V.; Ciardelli, F. *Polymer* **2002**, *43*,1115.
23. Tian, J. H.; Yu, W.; Zhou, C. X. *Polymer* **2006**, *47*, 7962.
24. Li, S. J.; Xiao, M. M.; Wei, D. F.; Xiao, H. N.; Hu, F. Z.; Zhang, A. N. *Polymer* **2009**, *50*, 6121.
25. Li, S. J.; Xiao, M. M.; Guan, Y.; Wei, D. F.; Xiao, H. N.; Zhang, A. N. *Eur. Polym. J.* **2012**, *48*, 362.
26. Zhai, W. T.; Wang, H. Y.; Yu, J.; Dong, J. Y.; He, J. S. *Polym. Eng. Sci.* **2008**, *48*, 1312.